Since January 2020 Elsevier has created a COVID-19 resource centre with free information in English and Mandarin on the novel coronavirus COVID-19. The COVID-19 resource centre is hosted on Elsevier Connect, the company's public news and information website.

Biosensors and Bioelectronics 213 (2022) 114436

Contents lists available at ScienceDirect

Biosensors and Bioelectronics

journal homepage: www.elsevier.com/locate/bios

An electrochemical aptasensor with N protein binding aptamer-complementary oligonucleotide as probe for ultra-sensitive detection of COVID-19

Mengdi Yu [a], Xiaohui Zhang [a], Xin Zhang [a], Qurat ul ain Zahra [d,e], Zenghui Huang [a], Ying Chen [a], Chunxia Song [a], Min Song [f], Hongjuan Jiang [f], Zhaofeng Luo [b,c,**], Ying Lu [a,*]

[a] Department of Applied Chemistry, Key Laboratory of Agricultural Sensors, Ministry of Agriculture and Rural Affairs, Anhui Agricultural University, Hefei, 230036, PR China
[b] School of Life Sciences, University of Science and Technology of China, Hefei, 230027, PR China
[c] The Cancer Hospital of the University of Chinese Academy of Sciences, Aptamer Selection Center, Institute of Basic Medicine and Cancer (IBMC), Chinese Academy of Sciences, Hangzhou, 310022, PR China
[d] Hefei National Lab for Physical Sciences at the Microscale and the Centers for Biomedical Engineering, University of Science and Technology of China, Hefei, 230026, PR China
[e] Core Facility Center for Life Sciences, Department of Molecular Biology and Cell Biology, University of Sciences and Technology of China, Hefei, 230026, PR China
[f] Affiliated Hospital of Anhui Agricultural University, Hefei, 230036, PR China

ARTICLE INFO

Keywords:
Electrochemical aptasensor
Rapid COVID-19 diagnosis
N protein detection
Regenerable aptamer sensor

ABSTRACT

The emergence of the COVID-19 epidemic has affected the lives of hundreds of millions of people globally. There is no doubt that the development of fast and sensitive detection methods is crucial while the worldwide effective vaccination programs are miles away from actualization. In this study, we have reported an electrochemical N protein aptamer sensor with complementary oligonucleotide as probe for the specific detection of COVID-19. The electrochemical aptasensor was prepared by fixing the double-stranded DNA hybrid obtained by the hybridization of N protein aptamer and its Fc-labeled complementary strand on the surface of a gold electrode. After incubation with the target, the aptamer dissociated from the labeled complementary DNA oligonucleotide hybrid to preferentially bind with N protein in the solution. The concentration of N protein was measured by detecting the changes in electrochemical current signals induced by the conformational transformation of the complementary DNA oligonucleotide left on the electrode surface. The sensor had a linear relationship between the logarithm of the N protein concentration from 10 fM to 100 nM ($\Delta I_p = 0.098 \log C_{N\ protein}/fM - 0.08433$, $R^2 = 0.99$), and the detection limitation was 1 fM (S/N = 3). The electrochemical aptamer sensor was applied to test the spiked concentrations of throat swabs and blood samples from three volunteers, and the obtained results proved that the sensor has great potentials for the early detection of COVID-19 in patients.

1. Introduction

The Corona Virus Disease 2019 (COVID-19) caused by severe acute respiratory syndrome coronavirus 2 (SARS-CoV-2) was reported at the end of 2019 (Chen et al., 2020; Guan et al., 2020; Huang et al., 2020a; Hui et al., 2020; Li et al., 2020; Lu et al., 2020; Wang et al., 2020a; Zhou et al., 2020). Health experts advised that an effective way to deal with the epidemic was by ensuring early detection, followed by isolation and treatment (Fraser et al., 2004; Hellewell et al., 2020; Kim et al., 2021; Tran et al., 2021; Wilder-Smith and Freedman, 2020). Increased survival rates and decreased risk of transmission are associated with the detection and treatments of victims during the latency period or the early stage of incidence. However, the viral load at this stage is usually too small to be detected. At present, the most commonly used detection method is qRT-PCR, which shows the technical issues related to high false-negative rates (Wang et al., 2020; Yelin et al., 2020; Zu et al., 2020). Electrochemical immunosensor assays (Eissa and Zourob, 2021; Li and Lillehoj, 2021; Tian et al., 2021) and lateral flow immunoassays

* Corresponding author.
** Corresponding author. School of Life Sciences, University of Science and Technology of China, Hefei, 230027, PR China
E-mail address: luy@ahau.edu.cn (Y. Lu).

https://doi.org/10.1016/j.bios.2022.114436
Received 30 November 2021; Received in revised form 24 May 2022; Accepted 27 May 2022
Available online 8 June 2022

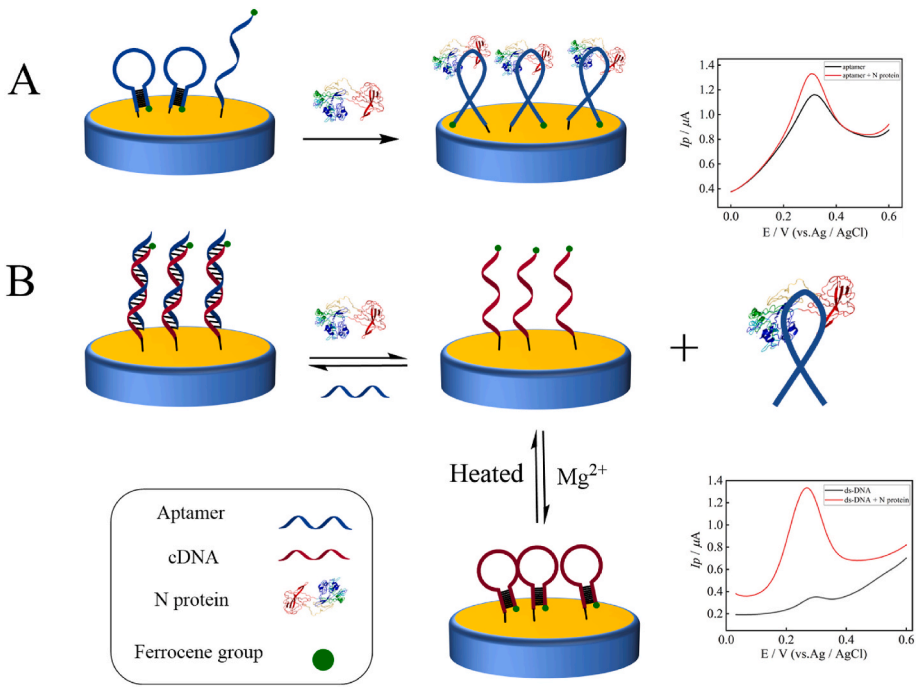

Scheme 1. Schematic diagram of the electrochemical aptasensor based on N protein-binding aptamer and Fc labeled complementary DNA oligonucleotide as probe. (A) Fc-labeled N protein aptamer conformation switching to a hairpin loop structure (before target incubation) and the change in conformation (after incubation with target). The change in the current signal is related to the Fc-electrode surface distance. (B) Incubation of ds-DNA hybrid (aptamer + Fc labeled complementary DNA oligonucleotide) with N protein. High affinity aptamer dissociated from the complementary DNA oligonucleotide to bind to the N protein, resulting in a stronger current signal change (related to the Fc-complementary DNA oligonucleotide structure switching to a hairpin loop) than strategy A.

(LFIAs) (Grant et al., 2020) have been developed for the detection of the SARS-CoV-2. However, the limit of detection (LOD) of these methods are normally at micromoles per liter, and the detection of virus traces in infected victims as early as possible is a critical factor for the epidemic prevention and control. Therefore, there is an urgent need for a more sensitive method towards COVID-19 detection.

SARS-CoV-2 has four main structural proteins, namely nucleocapsid protein (N protein), spike protein (S protein), membrane protein (M protein), and envelope protein (E protein) (Burbelo et al., 2020; Hassanzadeh et al., 2020; Wu et al., 2020, 2021; Xu et al., 2020; Zeng et al., 2020). As a major structural protein of coronavirus, the N protein plays an important role in packaging the RNA genome into helical ribonucleoproteins, modulating host cell metabolism, and regulating viral RNA synthesis during replication and transcription (Mu et al., 2020; Nelson et al., 2000; Stohlman et al., 1988). The N protein binds to the viral RNA genome, forming a long helical nucleocapsid structure or ribonucleoprotein (RNP) complex (Masters and Sturman, 1990). From in situ cross-linking and immunological experiments, it has been shown that RNP formation is essential for maintaining ordered RNA conformation suitable for viral genome replication and transcription (Tang et al., 2005). Due to the conservation of the N protein sequence and its high immunogenicity during infection, it is frequently used as a diagnostic and testing tool (Dutta et al., 2020). In the early stage of SARS infection, the detection sensitivity of N protein (90%) is higher than that of nucleic acid (42.9%), and the N protein in the serum samples of SARS patients can be detected as early as day 1 after the disease onset (Che et al., 2004; Li et al., 2005). Therefore, targeting the traces of N protein may play a critical role in COVID-19. In 2020, Professor Luo successfully screened N protein aptamer with a sequence of 5'-GCTGG ATGTC GCTTA CGACA ATATT CCTTA GGGGC ACCGC TACAT TGACA CATCC AGC-3' (Zhang et al., 2020a). The K_d value between the aptamer and N protein was determined to be 0.49 ± 0.05 nM. Electrochemical methods have the advantage of high sensitivity (Dong et al., 2019; Liu et al., 2017; Zhang et al., 2022). In our previous studies, electrochemical aptasensor was used to detect thrombin (5 pM) in the blood samples of ducks and ATP (0.5 nM) in the cerebrospinal fluid of rats (Zhang et al., 2018, 2020b). These works suggest that the N protein aptamer could be employed in electrochemical sensors for the early stage detection of N protein traces in throat swabs and blood samples of COVID-19 patients.

In conventional methods, the redox moiety labeled aptamers were often modified on the surfaces of electrodes and employed as probes (Liu et al., 2010; Yin et al., 2019). When targets induced aptamers are transformed from their relaxed conformations to hairpin or G-quadruplex, etc., the electrochemical current signals are also changed to indicate the concentration of targets. However, the N protein aptamer owns nine pairs of the complementary bases at both ends which could switch the aptamer to undergo a hairpin conformation without target-combination. Wang et al. confirmed that aflatoxin B1 aptamers with six pairs of complementary bases at both ends could not detect aflatoxin B1 through current signal change caused by conformational transition because it exhibits strong background signal at room temperature (Wang et al., 2020b). The actual conformation of the aptamer was possibly the hairpin structure as its melting temperature (T_m) was calculated to be 73.3 °C. In this work, we applied the redox moiety labeled N protein aptamer's complementary DNA oligonucleotide as probe. The ferrocene (Fc)-labeled single stranded DNA chain was modified on the electrode surface and hybridized with the unlabeled N protein binding aptamer. The rigid structure of the double-stranded DNA (ds-DNA) supported Fc away from the electrode surface, causing weak signal before detection. After target incubation, the aptamer was bound to the N protein target in the solution and dissociated from the complementary DNA oligonucleotide which transformed to a hairpin structure, hence the detection of the N protein was achieved by recording the changes in electrochemical current signal induced by the reduced distance between Fc and the electrode surface. In general, the findings of this work may be valuable in improving the delayed treatment-induced fatality rate of infections by providing a sensitive strategy for the early detection of COVID-19.

2. Experimental section

2.1. Chemicals and materials

Amylase (AMY), immunoglobulin G (IgG), hemoglobin (HGB), fibrinogen (FIB), cytochrome C, and thrombin were purchased from Beijing Soleibo Technology Co., Ltd. Sialomucin was provided by Shanghai yuanye Bio-Technology Co., Ltd. Myeloperoxidase (MPO), Azurocidin (AZU1), Neutrophil Elastase (ELANE), Myeloblastin

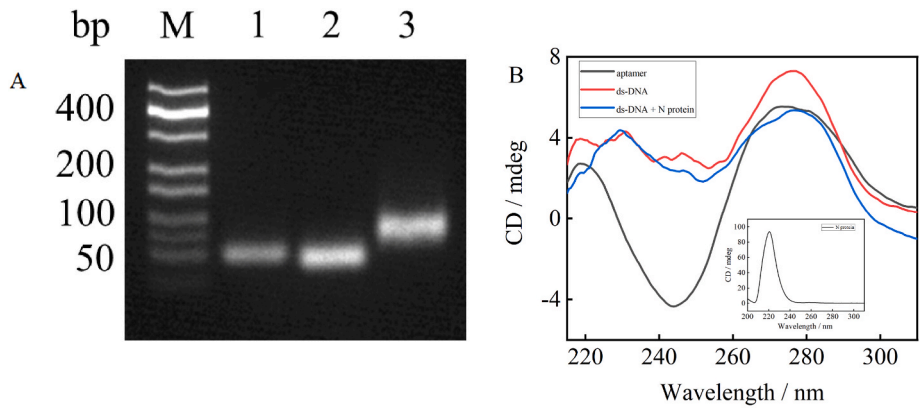

Fig. 1. (A) Agarose gel electrophoresis showing aptamer (lane 1), complementary DNA oligonucleotide (lane 2), and ds-DNA hybrid (lane 3). (B) CD spectra of aptamer (black curve), ds-DNA hybrid before (red curve) and after incubation with the target (blue curve) for 60 min at 25 °C. Inset: CD spectrum of N protein alone.

(PRTN3), and T4 polynucleotide kinase (T4 PNK) were purchased from Sangon Biotech (Shanghai, China) Co., Ltd. Bovine serum albumin (BSA) was supplied by Shandong sikejie Biotechnology Co., Ltd. Alkaline phosphatase (AKP) was provided by Shanghai Biyuntian Biological Co., Ltd. N protein was offered by Sino Biological Inc. All the DNA sequences were synthesized and purified by Sangon Biotech (Shanghai, China). The specific DNA sequences are shown in Table S1. All the solutions were prepared with ultra-pure water obtained from a Millipore water purification system (>18.2 MΩ·cm). All other chemicals used in this study were of analytical grade.

2.2. Apparatus and measurements

Cyclic Voltammetry (CV) and Differential Pulse Voltammetry (DPV) were measured by an electrochemical workstation (model CHI 660E, CHI Instruments, Shanghai, China). The three-electrode system consisted of an Au electrode (1.6 mm in diameter) which was modified with ds-DNA hybrid as the working electrode, Ag/AgCl (KCl-sat.) electrode as the reference electrode, and platinum wire as the auxiliary electrode. All measurements were performed in 20 mM Tris buffer containing 140 mM NaCl and 5 mM $MgCl_2$ at pH 7.6 (the optimization of the pH value of the Tris buffer is shown in Fig. S1 of **SI**).

3. Results and discussion

3.1. Principle of electrochemical detection

The schematic depiction of the designed electrochemical aptasensor in the current study is shown in Scheme 1 (A and B). The N protein aptamer was labeled with a redox moiety at one end, and modified on the electrode surface at the other end (SI, Table S1). By target incubation, the conformation of the aptamer switched and resulted to the electrochemical signal of redox moiety change. However, the aptamer of N protein had 9 pairs of complementary bases at both ends, which might form a hairpin structure before target detection. After incubation with the N protein target, the aptamer conformation changed in the resultant aptamer-target complex. As shown in Scheme 1A, the DPV value of only the electrode-modified aptamer was unsuitable for electrochemical sensor fabrication. We speculate that this may have been due to the distance between the electrode surface and the labeled redox group in the aptamer-target complex which did not change significantly compared to the distance in the hairpin loop structure.

In Scheme 1B we employed ferrocene (Fc)-labeled complementary DNA oligonucleotide of the N protein aptamer as probe (the cyclic voltammetry curves characterizing the Fc-labeled complementary DNA oligonucleotide are the adsorption control through different scanning rates are shown in Fig. S2 of SI). The label-free N protein-binding aptamer was hybridized with the labeled complementary DNA oligonucleotide to form ds-DNA hybrid, which was modified on the electrode surface by the addition of a thiol group at the other end of the complementary DNA oligonucleotide (SI, Table S1). When the N protein was incubated with the modified ds-DNA hybrid, the high affinity N protein-binding aptamer dissociated from the complementary DNA oligonucleotide to form an aptamer-target complex, while the conformation of the complementary DNA oligonucleotide single chain on the electrode surface changed to a hairpin structure in the presence of Mg^{2+}. Also, the distance between the Fc and the electrode surface was reduced, which induced changes in current signals. The measurement of the N protein concentration was achieved by recording the intensity of change in current signal. After target detection, the electrode was incubated with the label-free aptamer and heated to 95 °C. When the temperature was reduced to 20 °C at a speed of 1 °C/min, the aptasensor was regenerated with the formation of a ds-DNA hybrid on the electrode surface (the regeneration of the aptasensor is shown in Fig. S3 of SI).

3.2. Characterization of the aptasensor

To confirm the yield of the ds-DNA hybrid synthesis, we compared the agarose gel electrophoresis of the aptamer, complementary DNA oligonucleotide, and ds-DNA hybrid (The cyclic voltammetry characterization of the aptasensor is shown in Fig. S4). As shown in Fig. 1A, lane 1 shows a single-stranded aptamer, lane 2 represents single-stranded complementary DNA oligonucleotide, while lane 3 was obtained by annealing both single strand together. The analysis of the differences between the three lanes indicates that a double helical structure was formed with a yield of almost 100%. Fig. 1B shows the CD spectra of aptamer, ds-DNA hybrid, and the ds-DNA hybrid after incubation with the target for 60 min at 25 °C (the CD spectra of aptamer, ds-DNA hybrid, and ds-DNA hybrid after the incubation with the target at 40 °C and 80 °C are presented in Fig. S5 and Fig. S6, respectively). It can be seen from Fig. 1B that the peak of the ds-DNA hybrid (red curve) at 280 nm was significantly higher than that of the single stranded aptamer (black curve), and the peak value of the ds-DNA hybrid after target incubation (blue curve) was roughly equal to that of the single-stranded aptamer. N protein did not affect the results (inset in Fig. 1B). The changes in the peak values suggest that the ds-DNA hybrid was successfully dissociated into single-stranded after target incubation (the CD spectra of the aptamer at different temperatures are shown in Fig. S7; the CD of aptamer and complementary DNA oligonucleotide mixture before and after annealing process is shown in Fig. S8).

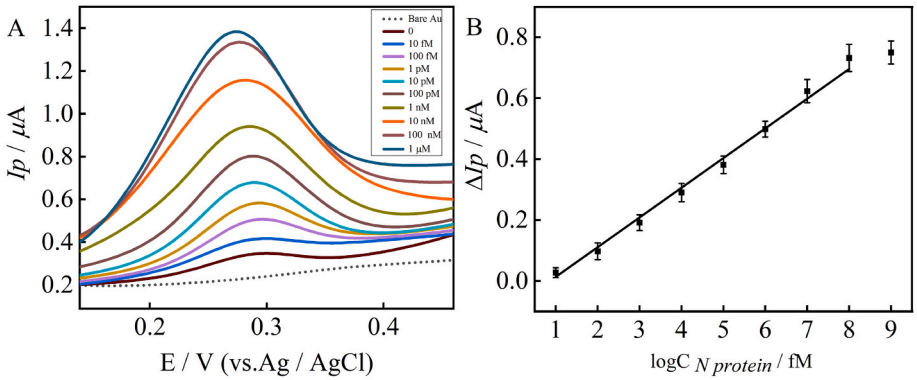

Fig. 2. (A) Differential pulse voltammetry (DPV) response signals recorded in Tris buffer. (B) The relationship between the logarithm of N protein concentration and ΔI_p value. The error bars indicate the standard deviations after three measurements.

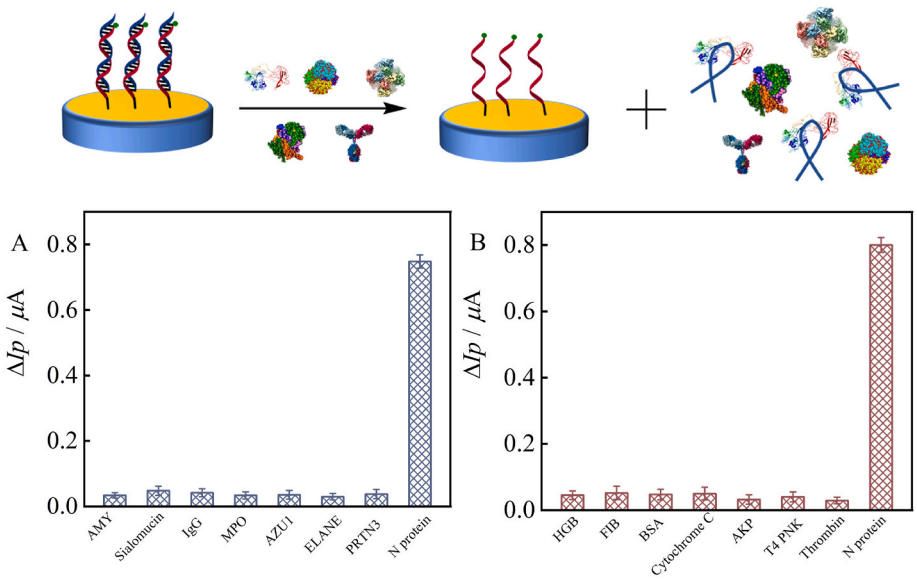

Fig. 3. Differential pulse voltammetry signals of several interferents in throat swabs (A) and human blood samples (B).

3.3. Analytical performance of the electrochemical aptasensor to N protein

To detect the concentration of the N protein by the aptasensor, the DPV signals were obtained by incubating the sensor with different concentrations of the N protein for 60 min (the optimizations of the reaction time of N protein, concentration of ds-DNA hybrid, and modification time of ds-DNA are shown in Fig. S9, Fig. S10, and Fig. S11; the cyclic voltammogram for the oxidative desorption of the ds-DNA monolayer from the Au surface is shown in Fig. S12). As shown in Fig. 2A, the dotted line represents the DPV response signal of the bare Au electrode, and the solid lines show the DPV signals after incubation with the N protein for 60 min. The concentrations of the N protein from bottom to top were 0, 10 fM, 100 fM, 1 pM, 10 pM, 100 pM, 1 nM, 10 nM, 100 nM, and 1 μM respectively. It is obvious that the DPV signals were enhanced by the increasing concentration of N protein target. Fig. 2B shows that ΔI_p ($\Delta I_p = I_p - I_{p0}$) had a linear relationship with the logarithm of the N protein concentration in the range of 10 fM to 100 nM ($\Delta I_p = 0.098 \log C_{N\ protein}/fM - 0.08433$, $R^2 = 0.99$), and the LOD was 1 fM (S/N = 3). The signal value at 1 μM was almost equal to that at 100 nM, implying that the sensor reached its maximum detection limit at 100 nM. Therefore, the concentration of the N protein can be calculated within the range of the linear relationship. The shelf-life of the sensor is tested to be about 96 h.

3.4. The selectivity of the aptasensor

Seven proteins commonly found in saliva were used as interferences to evaluate the selectivity of the aptamer sensor for N protein. Fig. 3A shows the ΔI_p values recorded in Tris buffer after the ds-DNA modified electrode was incubated with 1 μM AMY, 1 μM Sialomucin, 1 μM IgG, 1 μM MPO, 1 μM AZU1, 1 μM ELANE, 1 μM PRTN3 and 1 μM N protein for 60 min respectively. Compared with the N protein at a concentration of 1 μM, the ΔI_p signals of 1 μM AMY, 1 μM Sialomucin, 1 μM IgG, 1 μM MPO, 1 μM AZU1, 1 μM ELANE and 1 μM PRTN3 on the electrode accounted for 4.55%, 6.41%, 5.61%, 4.52%, 4.74%, 3.97%, and 5.03% respectively.

We also selected seven proteins commonly found in blood as interferences for selective experiments. Fig. 3B shows the ΔI_p values of ds-DNA modified electrode incubated with Tris buffer containing 1 μM HGB, 1 μM FIB, 1 μM BSA, 1 μM Cytochrome C, 10 U·mL^{-1} AKP, 10 U·mL^{-1} T4 PNK, and 1 μM thrombin, and 1 μM N protein respectively. Compared with 1 μM N protein, the ΔI_p signals of 1 μM HGB, 1 μM FIB, 1 μM BSA, 1 μM cytochrome C, 10 U·mL^{-1} AKP, 10 U·mL^{-1} T4 PNK and 1 μM Thrombin accounted for 5.63%, 6.5%, 5.88%, 6.25%, 4.0%, 5.01%, and 3.63% respectively. These results further confirm that the sensor can be used to specifically detect N protein in throat swabs and human blood samples.

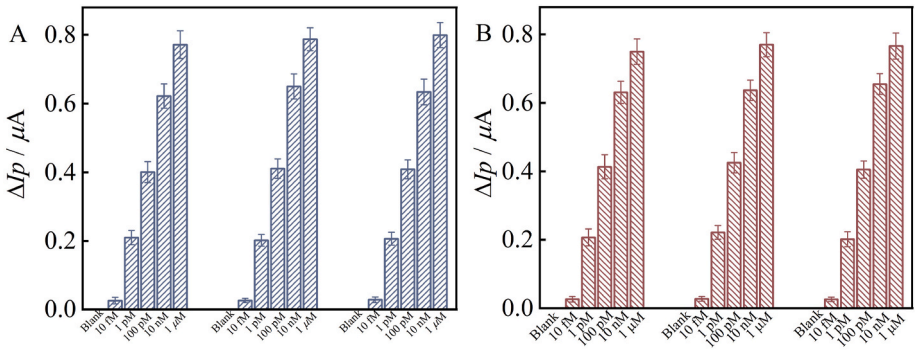

Fig. 4. (A) DPV values at different concentrations of N protein added to the throat swabs. (B) Determination of different concentrations N protein in blood samples.

Table 1
Recovery results of N protein in throat swabs and human blood samples.(n = 3).

Spiked (fM)	Throat swabs					Blood samples				
	Recovery (%)				RSD (%)	Recovery (%)				RSD (%)
	A	B	C	Average (%)		A	B	C	Average (%)	
10	94.1	96.3	103.7	98.0	30.0	98.3	103.0	97.3	99.5	27.0
1×10^3	109.9	105.8	108.2	108.0	9.0	108.2	116.0	105.5	109.9	10.6
1×10^5	105.2	107.9	107.3	106.8	7.1	108.6	111.7	106.4	108.9	7.2
1×10^7	99.8	104.3	101.8	102.0	5.7	101.3	102.2	105.1	102.9	4.8
1×10^9	102.9	105.0	106.6	104.8	4.6	99.9	102.7	102.2	101.6	4.8

3.5. Complex sample analysis of the aptasensor

The sample preparation processes are detailed in **SI**. We tried to test our electrochemical aptasensor's target detection efficiency with real samples. Three volunteers were randomly examined and their basic clinical features are displayed in Table S2 of **SI**. The throat swabs and blood samples of the three volunteers were taken an hour after breakfast, lunch, and dinner. The throat swabs were soaked in Tris buffer while the blood samples were not pretreated before detection. As shown in Fig. 4A and B, the blank samples and different concentration such as 10 fM, 1 pM, 100 pM, 10 nM and 1 μM of the N protein-added samples were tested. It can be seen that as the concentration of the added N protein target increased, the intensity of the electrochemical current signals also increased gradually. Therefore, the novel electrochemical aptasensor in the current study is expected to be effective for the early detection of COVID-19 in human bodies.

We used statistical method to obtain the average recoveries of the N protein from the throat swabs and blood samples. The recovery experiments were performed with N protein spiked at 10 fM, 1 pM, 100 pM, 10 nM, and 1 μM in throat swabs and blood samples. As shown in Table 1, the obtained recoveries of the throat swabs ranged from 98.0% to 108.0% and the RSD range was 4.6%–30.0%, while the recovery of the blood samples were in the range of 99.5%–109.9% with RSD from 4.8% to 27.0%. These results indicate that the reproducibility of the fabrication procedure of the sensor is remarkable, and the proposed method could be applicable for the measurement of N protein in real sample analysis.

4. Conclusion

In conclusion, we have constructed an electrochemical sensor based on the complementary DNA oligonucleotide of N protein binding aptamer as probe, which is expected to be ultra-sensitive for the detection of COVID-19 in real samples. In the concentration range of 10 fM to 100 nM, the electrochemical signal (ΔI_p) exhibited a linear relationship with the logarithm of the N protein concentration. The aptasensor exhibited a significant selectivity against N protein target among fourteen kinds of interference. This electrochemical aptamer sensor was applied to test the spiked N protein concentrations of throat swabs and blood samples from three volunteers. We look forward to obtaining permissions to test patients samples.

CRediT authorship contribution statement

Mengdi Yu: Investigation, Methodology, Data curation, Writing – original draft. **Xiaohui Zhang:** Investigation. **Xin Zhang:** Investigation. **Qurat ul ain Zahra:** Writing – review & editing. **Zenghui Huang:** Investigation. **Ying Chen:** Investigation. **Chunxia Song:** Funding acquisition. **Min Song:** Sample collection. **Hongjuan Jiang:** Sample collection. **Zhaofeng Luo:** Funding acquisition, Writing – review & editing. **Ying Lu:** Conceptualization, Supervision, Writing – review & editing.

Declaration of competing interest

The authors declare that they have no known competing financial interests or personal relationships that could have appeared to influence the work reported in this paper.

Acknowledgments

This work is financially supported by NSFC of China (Grant Nos. 21305002and 21705002) and the Fundamental Research Funds for the Central Universities (YD2070002016) and the Natural Science Foundation of Education Committee of Anhui Province (KJ2021A0176). The authors would like to thank all the reviewers who participated in the review, as well as MJEditor (www.mjeditor.com) for providing English editing services during the preparation of this manuscript.

Appendix A. Supplementary data

Supplementary data to this article can be found online at https://doi.org/10.1016/j.bios.2022.114436.

References

Burbelo, P.D., Riedo, F.X., Morishima, C., Rawlings, S., Smith, D., Das, S., Strich, J.R., Chertow, D.S., Davey, R.T., Cohen, J.I., 2020. J. Infect. Dis. 222, 206–213.

Che, X., Hao, W., Wang, Y., Di, B., Yin, K., Xu, Y., Feng, C., Wan, Z., Cheng, V.C.C., Yuen, K.Y., 2004. Emerg. Infect. Dis. 10, 1947–1949.

Chen, N., Zhou, M., Dong, X., Qu, J., Gong, F., Han, Y., Qiu, Y., Wang, J., Liu, Y., Wei, Y., Xia, J., Yu, T., Zhang, X., Zhang, L., 2020. Lancet 395, 507–513.

Dong, H., Zhou, Q., Zhang, L., Tian, Y., 2019. Angew. Chem. Int. Ed. 58, 13948–13953.

Dutta, N.K., Mazumdar, K., Gordy, J.T., 2020. J. Virol. 94 e00647-20.

Eissa, S., Zourob, M., 2021. Anal. Chem. 93, 1826–1833.

Fraser, C., Riley, S., Anderson, R.M., Ferguson, N.M., 2004. Proc. Natl. Acad. Sci. Unit. States Am. 101, 6146–6151.

Grant, B.D., Anderson, C.E., Williford, J.R., Alonzo, L.F., Glukhova, V.A., Boyle, D.S., Weigl, B.H., Nichols, K.P., 2020. Anal. Chem. 92, 11305–11309.

Guan, W., Ni, Z., Hu, Y., Liang, W., Ou, C., He, J., Liu, L., Shan, H., Lei, C., Hui, D.S.C., Du, B., Li, L., Zeng, G., Yuen, K.Y., Chen, R., Tang, C., Wang, T., Chen, P., Xiang, J., Li, S., Wang, J., Liang, Z., Peng, Y., Wei, L., Liu, Y., Hu, Y., Peng, P., Wang, J., Liu, J., Chen, Z., Li, G., Zheng, Z., Qiu, S., Luo, J., Ye, C., Zhu, S., Zhong, N., 2020. N. Engl. J. Med. 382, 1708–1720.

Hassanzadeh, K., Pena, H.P., Dragotto, J., Buccarello, L., Iorio, F., Pieraccini, S., Sancini, G., Feligioni, M., 2020. ACS Chem. Neurosci. 11, 2361–2369.

Hellewell, J., Abbott, S., Gimma, A., Bosse, N.I., Jarvis, C.I., Russell, T.W., Munday, J.D., Kucharski, A.J., Edmunds, W.J., Funk, S., Eggo, R.M., 2020. Lancet Global Health 8, e488–e496.

Huang, C., Wang, Y., Li, X., Ren, L., Zhao, J., Hu, Y., Zhang, L., Fan, G., Xu, J., Gu, X., Cheng, Z., Yu, T., Xia, J., Wei, Y., Wu, W., Xie, X., Yin, W., Li, H., Liu, M., Xiao, Y., Gao, H., Guo, L., Xie, J., Wang, G., Jiang, R., Gao, Z., Jin, Q., Wang, J., Cao, B., 2020. Lancet 395, 497–506.

Hui, D.S., Azhar, E.I., Madani, T.A., Ntoumi, F., Kock, R., Dar, O., Ippolito, G., McHugh, T.D., Memish, Z.A., Drosten, C., Zumla, A., Petersen, E., 2020. Int. J. Infect. Dis. 91, 264–266.

Kim, H.E., Schuck, A., Lee, S.H., Lee, Y., Kang, M., Kim, Y.S., 2021. Biosens. Bioelectron. 182, 113168–113173.

Li, Q., Guan, X., Wu, P., Wang, X., Zhou, L., Tong, Y., Ren, R., Leung, K.S.M., Lau, E.H.Y., Wong, J.Y., Xing, X., Xiang, N., Wu, Y., Li, C., Chen, Q., Li, D., Liu, T., Zhao, J., Li, M., Tu, W., Chen, C., Jin, L., Yang, R., Wang, Q., Zhou, S., Wang, R., Liu, H., Luo, Y., Liu, Y., Shao, G., Li, H., Tao, Z., Yang, Y., Deng, Z., Liu, B., Ma, Z., Zhang, Y., Shi, G., Lam, T.T.Y., Wu, J.T.K., Gao, G.F., Cowling, B.J., Yang, B., Leung, G.M., Feng, Z., 2020. N. Engl. J. Med. 382, 1199–1207.

Li, J., Lillehoj, P.B., 2021. ACS Sens. 6, 1270–1278.

Li, Y., Li, J., Liu, X., Wang, L., Li, T., Zhou, Y., Zhuang, H., 2005. J. Virol. Methods 130, 45–50.

Liu, W., Dong, H., Zhang, L., Tian, Y., 2017. Angew. Chem. Int. Ed. 56, 16328–16332.

Liu, Y., Tuleouva, N., Ramanculov, E., Revzin, A., 2010. Anal. Chem. 82, 8131–8136.

Lu, R., Zhao, X., Li, J., Niu, P., Yang, B., Wu, H., Wang, W., Song, H., Huang, B., Zhu, N., Bi, Y., Ma, X., Zhan, F., Wang, L., Hu, T., Zhou, H., Hu, Z., Zhou, W., Zhao, L., Chen, J., Meng, Y., Wang, J., Lin, Y., Yuan, J., Xie, Z., Ma, J., Liu, W.J., Wang, D., Xu, W., Holmes, E.C., Gao, G.F., Wu, G., Chen, W., Shi, W., Tan, W., 2020. Lancet 395, 565–574.

Masters, P.S., Sturman, L.S., 1990. Adv. Exp. Med. Biol. 276, 235–238.

Mu, J., Xu, J., Zhang, L., Shu, T., Wu, D., Huang, M., Ren, Y., Li, X., Geng, Q., Xu, Y., Qiu, Y., Zhou, X., 2020. Sci. China Life Sci. 63, 1–4.

Nelson, G.W., Stohlman, S.A., Tahara, S.M., 2000. J. Gen. Virol. 81, 181–188.

Stohlman, S.A., Baric, R.S., Nelson, G.N., Soe, L.H., Welter, L.M., Deans, R.J., 1988. J. Virol. 62, 4288–4295.

Tang, T.K., Wu, M.P.J., Chen, S.T., Hou, M.H., Hong, M.H., Pan, F.M., Yu, H.M., Chen, J. H., Yao, C.W., Wang, A.H.J., 2005. Proteomics 5, 925–937.

Tian, J., Liang, Z., Hu, O., He, Q., Sun, D., Chen, Z., 2021. Electrochim. Acta 387, 138553–138559.

Tran, V.V., Tran, N.H.T., Hwang, H.S., Chang, M., 2021. Biosens. Bioelectron. 182, 113192–113212.

Wu, A., Peng, Y., Huang, B., Ding, X., Wang, X., Niu, P., Meng, J., Zhu, Z., Zhang, Z., Wang, J., Sheng, J., Quan, L., Xia, Z., Tan, W., Cheng, G., Jiang, T., 2020. Cell Host Microbe 27, 325–328.

Wang, C., Horby, P.W., Hayden, F.G., Gao, G.F., 2020a. Lancet 395, 470–473.

Wang, C., Liu, L., Zhao, Q., 2020b. ACS Sens. 5, 3246–3253.

Wang, Y., Kang, H., Liu, X., Tong, Z., 2020. J. Med. Virol. 92, 538–539.

Wilder-Smith, A., Freedman, D.O., 2020. J. Trav. Med. 27, 1–4.

Wu, C., Qavi, A.J., Hachim, A., Kavian, N., Cole, A.R., Moyle, A.B., Wagner, N.D., Sweeney-Gibbons, J., Rohrs, H.W., Gross, M.L., Peiris, J.S.M., Basler, C.F., Farnsworth, C.W., Valkenburg, S.A., Amarasinghe, G.K., Leung, D.W., 2021. iScience 24, 102681–102698.

Xu, X., Chen, P., Wang, J., Feng, J., Zhou, H., Li, X., Zhong, W., Hao, P., 2020. Sci. China Life Sci. 63, 457–460.

Yelin, I., Aharony, N., Tamar, E.S., Argoetti, A., Messer, E., Berenbaum, D., Shafran, E., Kuzli, A., Gandali, N., Shkedi, O., Hashimshony, T., Mandel-Gutfreund, Y., Halberthal, M., Geffen, Y., Szwarcwort-Cohen, M., Kishony, R., 2020. Clin. Infect. Dis. 71, 2073–2078.

Yin, X., Hou, T., Huang, B., Yang, L., Li, F., 2019. Chem. Commun. 55, 13705–13708.

Zeng, W., Liu, G., Ma, H., Zhao, D., Yang, Y., Liu, M., Mohammed, A., Zhao, C., Yang, Y., Xie, J., Ding, C., Ma, X., Weng, J., Gao, Y., He, H., Jin, T., 2020. Biochem. Biophys. Res. Commun. 527, 618–623.

Zhang, L., Fang, X., Liu, X., Ou, H., Zhang, H., Wang, J., Li, Q., Cheng, H., Zhang, W., Luo, Z., 2020a. Chem. Commun. 56, 10235–10238.

Zhang, L., Zhang, X., Feng, P., Han, Q., Liu, W., Lu, Y., Song, C., Li, F., 2020b. Anal. Chem. 92, 7419–7424.

Zhang, X., Song, C., Yang, K., Hong, W., Lu, Y., Yu, P., Mao, L., 2018. Anal. Chem. 90, 4968–4971.

Zhang, Y., Ji, W., Zhang, S., Gao, N., Xu, T., Wang, X., Zhang, M., 2022. Angew. Chem. Int. Ed. 61, e202111853.

Zhou, F., Yu, T., Du, R., Fan, G., Liu, Y., Liu, Z., Xiang, J., Wang, Y., Song, B., Gu, X., Guan, L., Wei, Y., Li, H., Wu, X., Xu, J., Tu, S., Zhang, Y., Chen, H., Cao, B., 2020. Lancet 395, 1054–1062.

Zu, Z., Jiang, M., Xu, P., Chen, W., Ni, Q., Lu, G., Zhang, L., 2020. Radiology 296, E15–E25.